

Paper VII

Bulk-acoustic waves radiated from low-loss surface-acoustic-wave resonators

J. V. Knuuttila, J. J. Vartiainen, J. Koskela, V. P. Plessky,
C. S. Hartmann, and M. M. Salomaa

Reprinted with permission from J. V. Knuuttila, J. J. Vartiainen,
J. Koskela, V. P. Plessky, C. S. Hartmann, and M. M. Salomaa,
Applied Physics Letters, 84, 1579 (2004). Copyright 2004,
American Institute of Physics.

Bulk-acoustic waves radiated from low-loss surface-acoustic-wave resonators

J. V. Knuutila and J. J. Vartiainen

Materials Physics Laboratory, Helsinki University of Technology, P.O. Box 2200 (Technical Physics), FIN-02015 HUT, Finland

J. Koskela

Nokia Research Center, P.O. Box 407, FIN-00045 Nokia Group, Finland

V. P. Plessky

GVR Trade SA, Rue du Château 9, CH-2022 Bevaix, Switzerland

C. S. Hartmann

RFSAW, Inc., 900 Alpha Drive, Richardson, Texas 75081-6625

M. M. Salomaa^{a)}

Materials Physics Laboratory, Helsinki University of Technology, P.O. Box 2200 (Technical Physics), FIN-02015 HUT, Finland

(Received 8 September 2003; accepted 5 January 2004)

The bulk-acoustic conductance in low-loss surface-acoustic-wave filters utilizing leaky surface-acoustic waves is significant for the device operation. Here we directly measure the bulk acoustic wave radiation pattern on the backside of the piezoelectric substrate with the help of a scanning laser-interferometer probe. For the case studied, a leaky surface-acoustic wave resonator on $36^\circ\text{YX-LiTaO}_3$, a numerical calculation is carried out and the different bulk-wave modes arriving at the substrate bottom are identified by comparing the measured and computed energy-flow angles. The results are expected to lead to improved models for describing the operation of low-loss surface-acoustic-wave filters. © 2004 American Institute of Physics. [DOI: 10.1063/1.1650557]

The importance of bulk-wave radiation for low-loss radio frequency surface-acoustic-wave (SAW) filter performance is evident and the effect of bulk waves on the electrical response of leaky-SAW impedance-element filters was recently demonstrated.¹ Leaky surface-acoustic-wave (LSAW) resonators, used as the building blocks for impedance-element filters, radiate both slow shear bulk-acoustic waves (SSBAW) and fast shear bulk-acoustic waves (FSBAW). The resulting acoustic losses can be diminished by selecting a suitable crystal cut and/or metal thickness.^{2,3} However, some bulk-acoustic wave (BAW) radiation will always occur. Leakage into SSBAW modes results since the velocity of the LSAW is typically above that of the SSBAW velocity. In resonators or long interdigital transducer (IDT) structures, the slow shear bulk-acoustic waves are radiated into both the x and $-x$ directions and they propagate inside the substrate at an angle of $\sim 40^\circ$ for 36°-LiTaO_3 (see Fig. 1). On arrival at the bottom of the substrate, the SSBAWs are reflected off the substrate backside interface and subsequently propagate back to the top of the surface.

The fast shear bulk acoustic waves are also radiated but this typically occurs at frequencies above the leaky-wave stopband. Since the Bragg wave number of the grating is fixed, while the traveling FSBAW has a surface wave number which is increasing with f , it follows that the propagation angle for FSBAW strongly depends on frequency. Such FSBAW modes are relevant since LSAW resonators operate

only slightly below the cutoff frequency for the excitation of these waves.

Prior to this work, BAW radiation in SAW devices has been analyzed with the help of numerical methods⁴ including models for leaky surface waves.^{3,5-7} However, it has been difficult to verify some of the phenomenological modeling results since very little direct experimental data on the BAW radiation has been available. Direct measurements on the BAW fields generated in LiNbO_3 and LiTaO_3 crystals date back to the 1970's (Refs. 8-11) and provide no information on BAW radiation generated in the frequency range of modern LSAW resonators.

Here we report the direct experimental observation of the bulk-wave radiation, along with the energy-flow angles, at several frequencies measured with a specially constructed scanning laser-interferometric probe.¹² The interferometer features the high sensitivity of $10^{-4} \text{ \AA}/\sqrt{\text{Hz}}$, sufficient for probing LSAW up to $\sim 1.8 \text{ GHz}$. The lateral resolution of the measured field image is better than one micron.

The test resonator employed is a synchronous LSAW resonator on $36^\circ\text{YX-cut LiTaO}_3$ substrate. The sample has

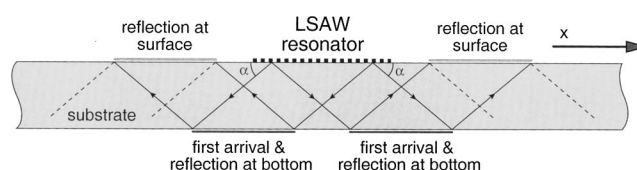


FIG. 1. Schematic for the SSBAW radiation path within the substrate in leaky SAW devices.

^{a)}Electronic mail: martti.salomaa@hut.fi

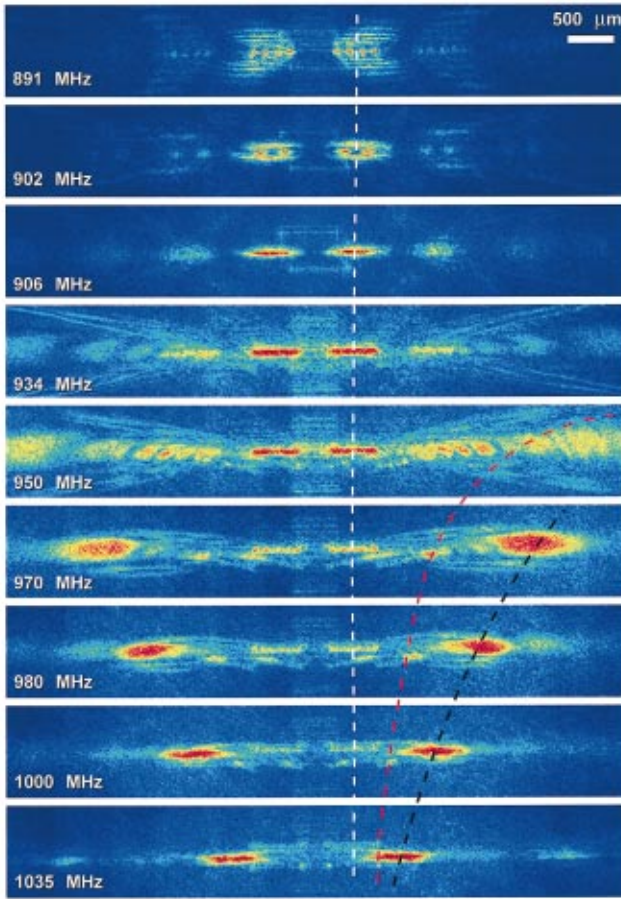


FIG. 2. (Color) Measured bulk-acoustic wave reflection patterns at the bottom surface of the SAW substrate.

120 electrode pairs in the IDT and a metallization ratio of 0.5.¹³ The sample is supported from the edges of the substrate in order to allow laser probing directly from the backside, i.e., the bottom of the substrate. However, special care is exercised to pin down the correct scanning location since the backside carries no information on the geometry of the device patterned on the top surface. Measured profiles are shown in the series of scans in Fig. 2. The resonator is located in the center of the image, but on the opposite side of the substrate. Each scan consists of 762 000 individual measurement points. The sample was not optimal for optical probing since the sand-blasted substrate bottom surface was rough. However, the high sensitivity of the interferometer and the addition of a thin reflecting graphite layer on the bottom surface enabled the adequate signal-to-noise ratio of 40 dB for the measurements.

At frequencies 906 MHz (resonance) and 934 MHz (antiresonance), the SSBW arriving at the substrate bottom are visible as two patterns of high amplitude. The second arrival of bulk-acoustic waves at the substrate bottom, though possessing weaker amplitudes, is also visible at 906 and 934 MHz. The energy-flow angle into the substrate varies only slightly. A white dotted line is shown in Fig. 2 to indicate the location of the first SSBW reflection occurring to the rhs.

Well above the stopband, at frequencies 970 MHz and 1 GHz, the images feature additional distinct patterns whose energy-flow angles strongly depend on frequency, shown in Fig. 2 with a black dotted line. They are identified as directly

excited FSBWs arriving at the bottom. In addition to these, careful analysis of the scanned images reveals another pair of yet weaker patterns, both consisting of two small spots shown in Fig. 2 with the dotted red line. The larger propagation angle of this radiation identifies it as the backward eigenmode-coupled FSBW. Interestingly, it occurs only at the reflectors. The contribution from the slow shear bulk-acoustic waves is still observed but it fades away for increasing frequencies.

At 950 MHz, continuous and semiperiodic patterns appear extending to the edges of the scanned area. These patterns have been identified as the first appearance of the backward eigenmode-coupled FSBW. The periodic structure is believed to be related to the finger structure, i.e., separate radiation from each individual reflector finger shows up as a separate pattern on the backside.

Radiation of bulk-acoustic waves by a resonator at frequency f is considered. Provided that the resonator is long and synchronous, it is well described by a long array of electrodes having the periodicity p . In a periodic array structure, bulk-acoustic waves are generated into discrete angles.¹⁴

Consider the following geometry. Let the direction of wave propagation on the surface be x and let the surface normal of the substrate be z . We assume all fields to be invariant along y , i.e., that the aperture is infinite. First consider a bulk-acoustic wave propagating in the substrate; its wave vector extends the angle θ with respect to the x axis. For any angle θ in a piezoelectric crystal, there can in general propagate three bulk-acoustic wave modes having the wave numbers $k_i(\theta) = 2\pi f/v_i(\theta)$, ($i = 1, 2$, and 3). The variation of the velocities as functions of the propagation direction are determined through the materials parameters for the substrate. Due to the anisotropy, the energy-propagation direction, Poynting vector, differs from k .

A periodic array of electrodes can radiate bulk-acoustic waves via three different mechanisms: (i) Direct excitation: Since the period of the voltage applied across the structure is $\lambda_0 = 2p$, the resonator generates waves for which the x component of the wave vector is a multiple of $2\pi/\lambda_0 = \pi/p$. A bulk-acoustic wave can be generated when the condition $k_i(\theta)\cos(\theta) = n\pi/p$ is fulfilled. In practice, when operating at

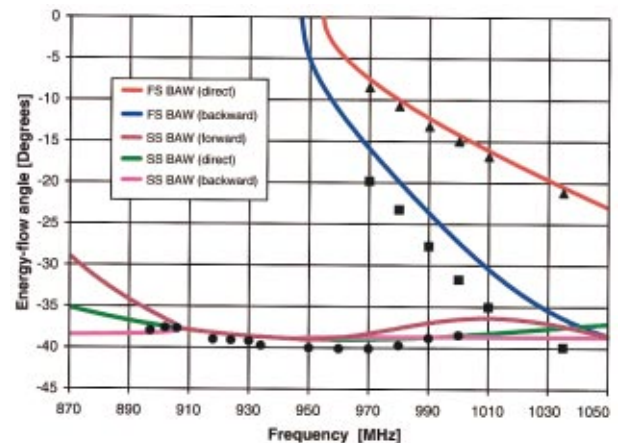


FIG. 3. (Color) Measured (distinct points) and calculated (continuous curves) values of the energy-flow angles for the various BAW radiation patterns.

the fundamental frequency, $n = \pm 1$. The x component of a bulk-acoustic wave can obtain all values in the range $|(k_i)_x| \leq 2\pi f / (v_i)_x|_c$, where $(v_i)_x|_c^{-1} = \max[\cos(\theta)/v(\theta)]$. Hence a bulk-acoustic wave mode i can be synchronously excited at all frequencies above the threshold value $(f_B)_i = (v_i)_x|_c/2p$. LSAW resonators usually operate at frequencies slightly below the threshold frequency for fast shear bulk-acoustic waves. Hence the SSBW is excited directly, while the FSBW is only excited above the threshold frequency. (ii) Eigenmode leakage and scattering into bulk-acoustic waves: In addition to the directly excited waves, there propagate eigenmodes in a resonator towards the left and right. Owing to reflections from the electrodes, the Fourier decomposition of the eigenmodes contains components for which the x component of the wave vector is of the form $\pm k_{\text{eig}} + nQ$, where n is an integer. The eigenmodes can couple to the bulk-acoustic waves, provided that the condition $k_i(\theta)\cos(\theta) = \pm k_{\text{eig}} + n2\pi/p$ is met. In practice, the cases $n=0, -1$ are involved at the fundamental frequency. In the case $n=0$, the eigenmode leaks into BAWs; for $n=-1$, the reflected eigenmode scatters into BAW. In a LSAW resonator, there occurs SSBW radiation owing to both of these mechanisms. In addition, in the vicinity of the threshold frequency, the eigenmodes start to be scattered into FSBW modes.

The emission angles for the direct excitation of BAW can be calculated with help of Peach's method, see Ref. 15. The Poynting vector was computed with the help of the x component of the wave vector and the materials parameters,¹⁶ and thereafter used to determine the energy-propagation direction.

The computation of the leakage of the eigenmodes and the scattering requires self-consistent solution of the dispersion equation. In the course of this procedure, the angles were estimated with the help of a simplified scheme: the value k_{eig} was computed numerically from the phenomenological Plessky dispersion equation¹⁷ as a function of frequency. The parameters of the model were determined by matching to the electric response of the resonator. Finally, the Peach method was employed, just like in the case of direct excitation.

The experimental energy-flow angles for each mode are calculated using the known substrate thickness (345 μm) and the location of each pattern on the substrate backside. The measured results are compared in Fig. 3 with theoretically calculated curves. From the results, three different BAW-excitation mechanisms can be identified: (i) directly excited BAW (slow shear, fast shear for $f > 955$ MHz); (ii) forward eigenmode-coupled BAW (slow shear); and (iii) backward eigenmode-coupled BAW (slow shear, fast shear for $f > 947$ MHz).

The minor discrepancies in Fig. 3 between the calculated and experimental results are attributed to the approximations used in the computations, especially concerning the backward eigenmode-coupled FSBW. Also, the experimental values exhibit a small (~ 1 MHz) downward frequency shift, due to the elevated temperature induced by the high input power used (21 dBm).

Direct measurements of the various BAW components radiated by leaky SAW resonators have been presented. We give the quantitative comparison between the experimentally determined energy-flow angles and the theoretically modeled values for such a structure. The leakage phenomena associated with bulk-acoustic waves are significant for SAW impedance-element filters designed for mobile-communication applications. Our results are expected to aid in developing improved low-loss device designs.

Jaakko Saarinen is acknowledged for help with the sample preparation and measurements. J.J.V. thanks the Foundation of Technology (TES, Finland) for a scholarship. This research has been supported by the Graduate School for Technical Physics and the Academy of Finland.

- ¹S. N. Kondratiev and T. Thorvaldsson, *Proceedings of the IEEE Ultrasonics Symposium 1999* (IEEE, New York, 1999), p. 317.
- ²O. Kawachi, S. Mineyoshi, G. Endoh, M. Ueda, O. Ikata, K. Hashimoto, and M. Yamaguchi, *IEEE Trans. Ultrason. Ferroelectr. Freq. Control* **48**, 1442 (2001).
- ³J. Koskela, V. P. Plessky, and M. M. Salomaa, *IEEE Trans. Ultrason. Ferroelectr. Freq. Control* **45**, 439 (1998).
- ⁴K. C. Wagner, L. Reindl, and O. Männer, *Proceedings of the IEEE Ultrasonics Symposium 1993* (IEEE, New York, 1993), p. 209.
- ⁵V. P. Plessky, D. P. Chen, and C. S. Hartmann, *Proceedings of the IEEE Ultrasonics Symposium 1994* (IEEE, New York, 1994), p. 297.
- ⁶K. Hashimoto, M. Yamaguchi, G. Kovacs, K. C. Wagner, W. Ruile, and R. Weigel, *IEEE Trans. Ultrason. Ferroelectr. Freq. Control* **48**, 1419 (2001).
- ⁷K. J. Gamble and D. C. Malocha, *IEEE Trans. Ultrason. Ferroelectr. Freq. Control* **49**, 47 (2002).
- ⁸T. Chiba and Y. Togami, *Appl. Phys. Lett.* **29**, 793 (1976).
- ⁹Y. Togami and T. Chiba, *J. Appl. Phys.* **49**, 3587 (1978).
- ¹⁰W. S. Goruk and G. I. Stegeman, *Appl. Phys. Lett.* **32**, 265 (1978).
- ¹¹J. Melngailis, H. A. Haus, and A. Lattes, *Appl. Phys. Lett.* **35**, 324 (1979).
- ¹²J. V. Knuutila, P. T. Tikka, and M. M. Salomaa, *Opt. Lett.* **25**, 613 (2000).
- ¹³J. Koskela, J. V. Knuutila, T. Makkonen, V. P. Plessky, and M. M. Salomaa, *IEEE Trans. Ultrason. Ferroelectr. Freq. Control* **48**, 1517 (2001).
- ¹⁴In an actual finite device, this is not the case, but one may assume the bulk-acoustic wave radiation to concentrate around these directions.
- ¹⁵R. C. Peach, *Proceedings of the IEEE Ultrasonics Symposium 1995* (IEEE, New York, 1995), p. 221.
- ¹⁶G. Kovacs, M. Anhorn, H. E. Engan, G. Visintini, and C. C. W. Ruppel, *Proceedings of the IEEE Ultrasonics Symposium 1990* (IEEE, New York, 1990), p. 435.
- ¹⁷V. P. Plessky, *Proceedings of the IEEE Ultrasonics Symposium 1993* (IEEE, New York, 1993), p. 195.